Various approaches of energy estimation of giant air showers

L.G. Dedenko[a]*, D.A. Podgrudkov[a], G.P. Shoziyoev[a],
T.M. Roganova[b], G.F. Fedorova[b], E.Ju. Fedunin[c]
[a] *Physical Department of Moscow State University*
Moscow 119992, Leninskie Gory, Russia
[b] *Skobeltsyn Institute of Nuclear Physics of Moscow State University*
Moscow 119992, Leninskie Gory, Russia
[c] *Research-Development Center REAGENT*
Moscow 125190, ul. Kosigina 4, Russia

Abstract

New estimates of energy of giant air showers have been simulated both by the CORSIKA code with the thinning level of 10^{-6} and by our modified multilevel scheme in terms of the quark-gluon string model. Both approaches use the GEANT4 code to simulate the responses of scintillation detector stations in giant air showers. These new estimates show approximately 1.7 lower energies of giant air showers for a given signal $s(600)$ in comparison with the standard approach used at the Yakutsk array. If these new estimates of energy are accepted then the intensity of giant air showers observed at the Yakutsk array would be approximately the same as observed by the HiRes Collaboration. Simulations of the Cherenkov radiation are in agreement with data observed at the Yakutsk array if the value of the signal $s(600)$ is ignored. But for fixed value of signal $s(600)$ simulations show lower number of Cherenkov photons. The simulations of the fluorescence light production show rather wide lateral distributions.

1 Introduction

The Greizen-Zatsepin-Kuzmin effect (GZK) [1], [2] is the very peculiar feature of the energy spectrum of the primary cosmic rays (PCR) at energies above $\sim 5 \times 10^{10}$ GeV. The interactions of the primary protons and nuclei with the microwave background radiation should decrease considerably the number of the primary particles which may reach the atmosphere of the Earth with such huge energies. It is the famous cutoff of the energy spectrum predicted many years ago [1], [2]. The observations made at the Yakutsk Array (YA) [3] and at the Akeno Giant Air Shower Array (AGASA) [4] seem to contradict this prediction. However, observations by the High Resolution Array (HiRes) [5] do support the GZK effect. The Pierre Auger Observatory (PAO) Collaboration [6] can now not support nor reject the data [5] because of very large errors ($\sim 50\%$) of energy estimates. Many approaches have been suggested to find out energy estimates. The standard estimate of energy of extensive air showers (EAS) is based on the signal in scintillation detectors or water tanks caused by shower particles. This estimate depends much on the model of the hadronic interactions at superhigh energies and composition of the PCR. So it is better to use such parameters of EAS which are more robust and do not depend much on any model suggestions. At the YA the Cherenkov radiation have been used to calibrate signals in scintillation detectors. The HiRes Collaboration exploits only the fluorescence light to measure energy of EAS. The PAO Collaboration calibrated signals in water tanks with help

* **e-mail**: ddn@dec1.sinp.msu.ru

of the fluorescence light. The multilevel scheme [7], [8] has been suggested to estimate signals in scintillation detectors (a density of energy deposited in scintillator by shower particles). The crucial element of this scheme is a creation of the library of signals caused by cascades in the atmosphere with energies below some threshold. Such calculations can be carried out with help of the CORSIKA [9] and GEANT4 [10] codes. These calculations may be extended to include simulations of the Cherenkov radiation and the fluorescense light production in the atmosphere. Then the source functions which describe the production of these low energy particles in the atmosphere should be calculated with the help of the CORSIKA code. Finally, distributions of signals in scintillation detectors, Cherenkov detectors and fluorescense light detectors should be simulated. In this paper some results concerning lateral distributions of these signals in various detectors are presented. Besdes, the possibility to detect the primary photons are also analysed.

2 Lateral distributions of signal s(r)

The high energy particles move mainly in one direction while the low energy particles spread in the 3-dimensional space. So it is possible to suggest an approximation when all possible movements are divided into these two categories. To separate these two regimes the threshold energy E_{thr} may be introduced. For electrons and gammas the value of E_{thr} may be chosen as 10 GeV while for muons it should be above 10^3 GeV. So within this adopted approximation particles with energies above the threshold energy E_{thr} are regarded as high energy particles. The low energy particles with energies under the value of E_{thr} can be produced anywhere in the atmosphere. The main advantage of this scheme is that the electron-photon cascades produced in the real atmosphere by these low energy particles may be simulated once and forever because the cross sections of the physical processes involved are well known. Moreover, for every cascade induced by any low energy particle in the atmosphere the responses of detectors may be also estimated as energies and the zenith angles of every secondary particle which reaches the level of observation and strikes a detector are known. These simulations of low energy cascades initiated by electrons and gammas with various energies for different starting points in the real atmosphere and responses of detectors may be carried out in advance to create the library of responses (LR). So this approach enable us to have the lateral distributions of signals $SE(r, E_i, x_k)$ and $SG(r, E_i, x_k)$ produced in scintillation detectors due to cascades initiated by electrons and gammas respectively with energy E_i and generated at depth x_k. Note, that the energy E_i is inside the interval $0.001 \leq E_i \leq 10$ GeV, $(i = 1, \ldots, 11)$ and depth x_k is inside the interval $0 \leq x_k \leq 1020$ g/cm^2 $(k = 1, \ldots, 21)$. It should be mentioned that this library does not depend on model of hadronic interactions and mass composition. We have used the CORSIKA (EGS4) code [9] and GEANT4 code [10] to create this LR. For any electron or gamma generated with energy E at the depth x responses of detectors may be estimated by simple interpolation with the LR data. So all we need to simulate the signals for the real air shower is a knowledge of production rate of these low energy electrons and gammas, or source functions $S_e(E, x)$ and $S_\gamma(E, x)$. These functions have a simple meaning: $S_e(E, x)dEdx$ and $S_\gamma(E, x)dEdx$ are numbers of electrons with energy E and gammas respectively generated at depth x. Due to original suggestions of the multilevel scheme [7], [8] the equations which describe the transport of the high energy particles should be solved to calculate these source functions $S_e(E, x)$ and $S_\gamma(E, x)$. Then a signal at distance r induced by electrons and gammas in an extensive shower may be estimated:

$$SEG(r) = \int dE \int dx (SE(r, E, x) \cdot S_e(E, x) + SG(r, E, x) \cdot S_\gamma(E, x)). \tag{1}$$

Here signals $SE(r, E, x)$ and $SG(r, E, x)$ may be calculated by simple interpolation with the help of the library of responses LR.

But it is possible to use any other approach, e.g. simulations with help of the CORSIKA code. In a standard mode of the CORSIKA running all particles with energies below E_{thr} are disregarded. So we have to make some modifications of this standard mode to be able to sample such electrons and photons in specially created files $S_e(E_i, x_i, w_i)$ and $S_\gamma(E_j, x_j, w_j)$ respectively. Here E_i and E_j are energies of electrons and photons; x_i and x_j are points of their generation in the atmosphere and w_i and w_j are weights assigned to particles due to the thinning procedure used. Integers i and j are changing from 1 up to N_e and N_γ - the total numbers of electrons and gammas respectively created with help of the CORSIKA code in the extensive air shower. Because the value of energy E_{thr} is rather high the weights w_i and w_j are not very large. So we do not expect that the artificial fluctuations would be considerable. For muons we chose $E_{thr} = 0.3$ GeV. The transport of these muons was simulated up to the observation level and then the GEANT4 code was used to estimate the signal $SM(r)$ in a detector at distance r from the shower axis. The total response of detector was a sum of signals produced by all particles:

$$s(r) = \sum_{i=1}^{N_e} w_i \cdot SE(r, E_i, x_i) + \sum_{j=1}^{N_\gamma} w_j \cdot SG(r, E_j, x_j) + SM(r). \tag{2}$$

The calculations carried out for vertical showers with energies 10^9, 10^{10} and 10^{11} GeV gave the following formula for estimating energy E for given value of the signal $s(600)$:

$$E = 3 \cdot 10^8 \cdot s(600)^{0.99}, GeV. \tag{3}$$

This estimate is nearly 1.6 times less than the standard approach used at the YA [3].

As for the inclined showers we think it is better not to use the zenith angle dependence of the signal estimated by the equal-intensity cuts method but rather to calculate the lateral distribution of this signal in the detector plane which will have no azimuthal symmetry. Then estimate of energy may be obtained by comparison of the data with the simulated distribution.

To be sure that our simulations are correct we have carried out calculations for the AGASA detector and found the estimate:

$$E_0 = 2 \cdot 10^8 \cdot s(600), GeV, \tag{4}$$

which is in nice coincidences with the AGASA results [4]. Fig.1 shows our results (points) and the approximation used in [4] (solid line). So our simulations gave a full support to the AGASA estimates of energy for the vertical showers but differ by a factor of 1.6 with the estimates used at the YA [3]. But the signal $s(600)$ at the YA have been calibrated with help of the Cherenkov radiations which we should take into account.

3 Calculations of the Cherenkov radiation

Similarly to calculations of distributions of signal $s(r)$ first the library of lateral distribution functions (LDFL) $CE(r, E_i, x_k)$ and $CG(r, E_i, x_k)$ of Cherenkov radiation within 300-800 nm which falls on detector inside the angle of 55^o for the electron-induced and gamma-induced cascades has been simulated. The distance r from the shower axis can vary from 5 to 1000 m, energies of electrons and gammas were inside the interval $0.02 \leq E_i \leq 10$ GeV (10 points) and we had 21 points x_k where the cascades start to develop from. The lateral distribution function of Cherenkov radiation in an air shower may be estimated with help of the introduced above source functions $S_e(E_i, x_i, w_i)$ and $S_\gamma(E_j, x_j, w_j)$:

$$c(r) = \sum_i w_i \cdot CE(r, E_i, x_i) + \sum_j w_j \cdot CG(r, E_j, x_j). \tag{5}$$

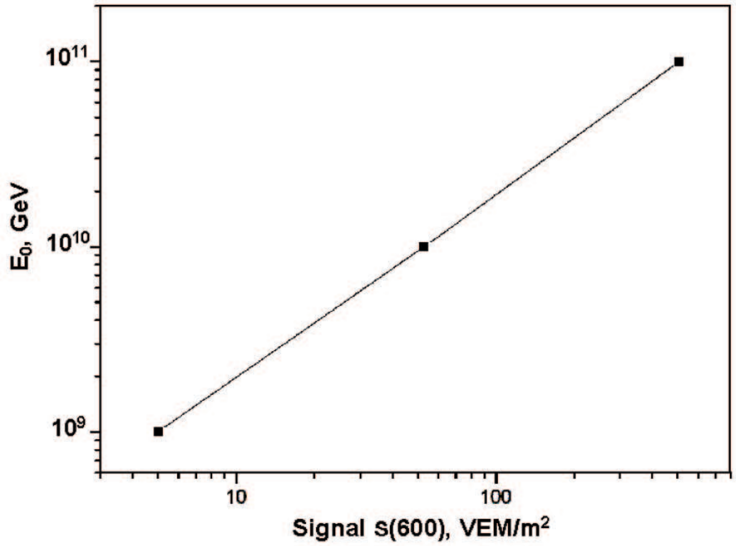

Figure 1: Dependence of energy E_o on the signal $s(600)$. Solid line - [4], points - our results

Here functions $CE(r, E_i, x_k)$ and $CG(r, E_i, x_k)$ are calculated from the created library LDFL by simple interpolations. Fig.2 illustrates distributions (5) calculated for showers with energies 10^9, 10^{10} and 10^{11} GeV (curves 1 - 3, respectively). These distributions coincides with approximation used at the YA [11].

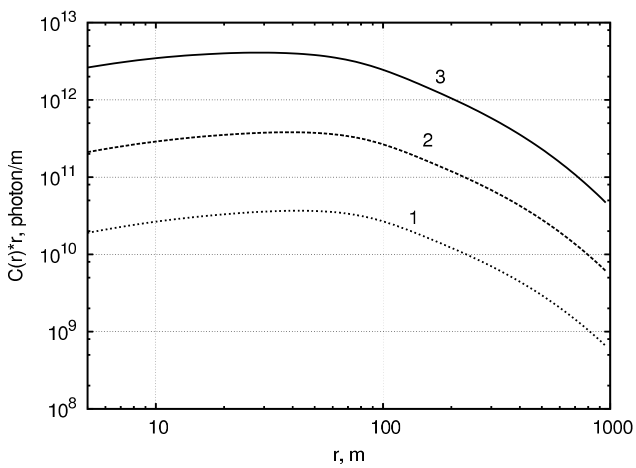

Figure 2: Lateral distributions of Cherenkov light. Curves: 1 - 10^9, 2 - 10^{10}, 3 - 10^{11} GeV

In terms of the QGSJET01 model [12] with the help of the CORSIKA code we have estimated the dependence of the density of Cherenkov photons at 400 m from shower axis on the signal $s(600)$:

$$c(400) = 3.4 \cdot 10^7 \cdot s(600)^{0.99}. \tag{6}$$

Because calculated values of signals $s(600)$ are lager then the YA data show this formula (6) gives ~ 1.7 times smaller density of photons. So we have to understand how to explain this difference. If experimental values are accepted then we have to change a model of hadronic interactions or to take heavier primary composition. But with calculated values of the signal $s(600)$ the intensity of the energy spectrum observed at the YA may be decreased so that the good agreement with the HiRes spectrum would be reached. Thus, more study is needed. On the other hand the production of the fluorescence light should also be understood.

4 Lateral distribution of energy deposition by particles in the atmosphere in extensive air showers

As there are now some uncertainties in the fluorescence light yield [13] and because the fluorescence light production depends on the particular parameters of the atmosphere we had confined ourselves by calculations of energy deposition by shower particles in the standard atmosphere. The solution of this problem depends on the physical processes at the very low energies. So we have to use the GEANT4 code which provides much lower values of threshold energy of secondary particles than the CORSIKA code does. First for electrons and gammas with energies E_i from interval of 0.001-10 GeV ($i = 1, \ldots, 30$) the vertical electron-photon cascades from the starting points x_k ($0 \le x_k \le 1040$ g/cm^2, $k = 1, \ldots, 40$) up to the level of observation $x_0 = 1040$ g/cm^2 have been simulated and energy depositions ΔE in the ring volumes with radii R_j and R_{j+1} ($0 \le R_j \le 2000$ m, $j = 1, \ldots, 100$) and with a heigth of $h_m = 50$ m ($1 \le m \le 1000$) have been calculated. The total number of simulated cascades was $N \sim 0.24 \cdot 10^9$. So the library of energy depositions was calculated. As a more simple but less detailed approach the energy depositions $\Delta E(E_i, x_j, r_k, h_m)$ in small cylindrical rings with heights $h_m = 50$ m may be summed to find out such depositions in large cylindrical rings with height of 50 km:

$$\Delta E(E_i, x_j, r_k) = \sum_{m=1}^{1000} \Delta E(E_i, x_j, r_k, h_m). \tag{7}$$

Fig.3 shows distributions (7) for electrons (solid lines) and gammas (dotted lines) with energy of 10 GeV for cascades which have been generated at depths 872, 636 and 0 g/cm2 (curves 1 -3, respectively). Fig.4 shows fractions of energy deposition by electrons (solid curves) and gammas (dotted curves) with energy $E_0 = 10$ GeV inside the cylinder with radius r as functions of this radius r for cascades generated at depths 872, 636 and 0 g/cm2 (curves 1 -3, respectively).

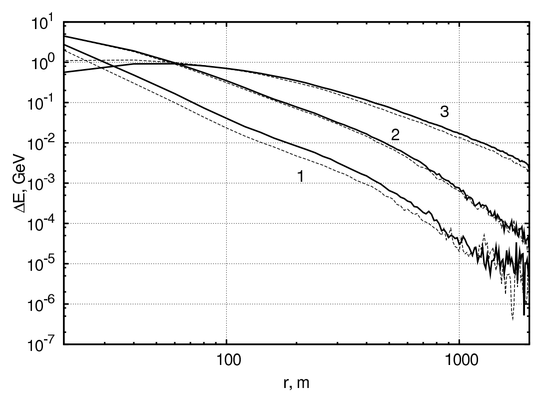

Figure 3: Lateral distributions of the fluorescent light. Solid lines - electrons, dotted lines - gammas. Curves: 1 - 872 g/cm^2, 2 - 636 g/cm^2, 3 - 0 g/cm^2

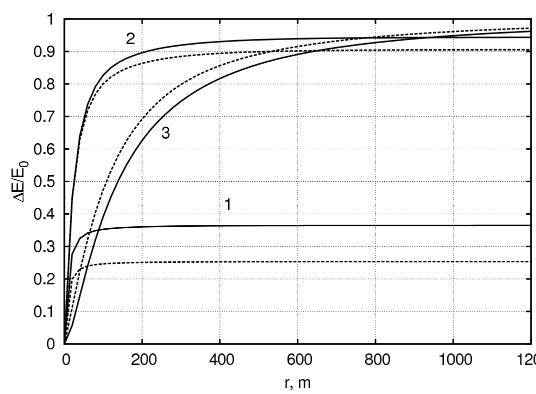

Figure 4: Fraction of deposited energy inside the cylinder with radius r. Curves 1, 2, 3 as in Fig3

Even if some heights h_m are happened to be above the starting level x_j the sum (7) has a sense because the backscattered particles (the backward current) should be taken into account at small energies of secondary particles. The energy depositions in such large cylindrical rings in extensive air shower may be estimated with help of a scheme already used above:

$$\Delta E(r_k) = \sum_i w_i \Delta E_e(E_i, x_i, r_k) + \sum_j w_j \Delta E_\gamma(E_j, x_j, r_k). \tag{8}$$

Here $\Delta E_e(E_i, x_i, r_k)$ and $\Delta E_\gamma(E_j, x_j, r_k)$ are sums (7) estimated for electrons and gammas respectively. Finally, lateral distribution of deposited energy may be calculated:

$$\rho_{\Delta E}(r_k) = \Delta E(r_k)/\pi(r_k^2 - r_{k-1}^2). \tag{9}$$

Note that for $k = 1$ it is not a ring but a cylinder. Due to energy conservation the sum

$$\Delta E = \sum_k \Delta E(r_k). \tag{10}$$

should be equal to the energy deposited to the source functions.

We can see from Fig.4 that nearly 30-40% of the energy may be deposited at distance above 100 m from the shower axis. These values should be compared with estimation $\geq 10\%$ found with help of the CORSIKA code [14]. Because a typical value of the viewing angle at which fluorescence light is collected is $\sim 1.3^o$ due to the procedure of maximizing the signal to noise ratio this "missing" energy should be taken into account. Besides, due to the backward current some fractions of deposited energy may be delayed. In inclined showers this distribution of the deposited energy should be even broader because the shower maximum position will be higher in the atmosphere. We hope that signals in the scintillation detector and the fluorescence light production in EAS should be understood in terms of the same model of hadronic interactions and the same mass composition.

5 The primary photons

It is not excluded yet that some of the primary particles at ultrahigh energies may be the primary photons. Thus we should be able to analyze also the properties of gamma-induced air showers. At energies above $\sim 10^{18}$ eV both interactions of the primary photons with the geomagnetic field outside of the atmosphere [15] and Landau-Pomeranchuk-Migdal (LPM) effect [16] should be taken into account. As in interactions with the geomagnetic field a large number of secondary particles are produced the role of the LPM effect is reduced considerably though both effects may be studied separately. The technique of adjoined cascade equations has been suggested to study the gamma-induced showers [17]. The CORSIKA code with the option of the "preshower" mode has been also used [18]. The approach with usual cascade equations in the integral form has been also suggested [19]. Here we have used this approach to estimate muon density at distance of 1000 m from the shower axis to be able to distinguish the gamma-induced showers from the proton ones. In first simplified version we have used the standard approximation A of the cascade theory for the cross section of the bremshtralung and pair production processes. As above the value of the threshold energy E_{thr} was 10 GeV. The source functions $S_e(E, x)$ and $S_\gamma(E, x)$ of the electrons and gammas with energies below 10 GeV have been estimated as a result of the solution of the transport equations.

We have suggested to use the integral form of the transport equations for electrons and gammas to find out their solution. The accuracy of this solution can be checked with help of the energy balance. Fig.5 shows this balance in a shower induced be the primary photon with energy $E_0 = 10^{10}$ GeV. The curve 1 shows how the fraction of energy carried by this photon decreases with depth t. The curves 2 and 3 illustrate how energies carried by secondary electrons and photons (in units of E_0) and their sum (curve 5) change with depth t. The energy transported beyond the threshold $E_{thr} = 10$ GeV (also in units of E_0) is shown by the curve 4. The curve 6 shows the total balance of energy in a shower. We can see that within a few per cent the total energy in a shower is conserved. It should be mentioned that the cross sections for the pair production and for the bremstrahlung processes were used in approximation A of the cascade theory. As our approach allows to use any cross sections we have used also the Migdal cross sections to take into account the Landau-Pomeranchuk-Migdal effect (LPM) [16].

Fig.6 shows one hundred individual cascade curves for showers with energy of 10^{11} GeV (solid lines) and their average (solid circles) when the LPM effect taken into account. Asterisks

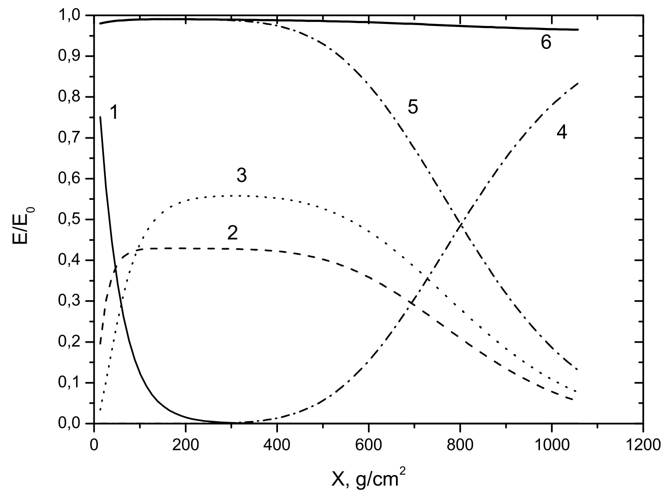

Figure 5: Energy balance (in fractions of E_0) in gamma-induced shower. Curves: 1 - primary photon, 2 - electrons, 3 - gammas, 4 - under threshold, 5 - sum of 2 and 3, 6 - total balance

show the Bethe-Gaitler (BG) cascade curve. What is important, it is large fluctuations in development of individual cascades. Finally, Fig.7 shows the muon density at a distance of 1000 m from the shower axis in gamma induced showers with various energies. Results for the average LPM showers are shown by solid line. Black circles show 10 individual results for $E_0 = 10^{11}$ GeV. Again one can see huge fluctuations due to the LPM effect. Dotted line shows result for the BG cross section. One can see a noticeable difference. Black square shows results by [17].

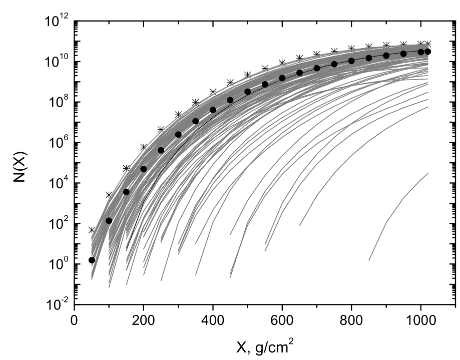

Figure 6: Cascade curves for the gamma-induced showers with $E_0 = (10)^{11}$ GeV. Solid lines - with the LPM, asterixes - BG shower, solid circles - average of LPM curves

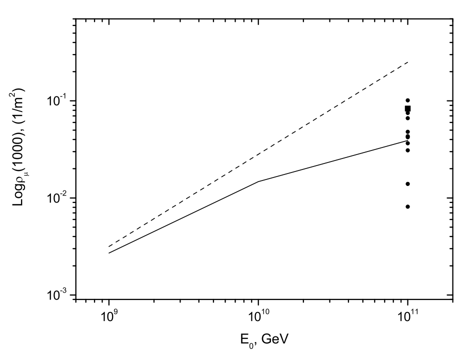

Figure 7: Dependence of muon density at 1000 m from the shower axis. Dotted line - BG showers, solid line - LPM showers, solid circles - LPM individual showers, black square - [17]

6 Conclusion

Calculations in terms of the QGSJET01 [12] model show energy estimates which by a factor of 1.6-1.7 less than used at the YA. Simulations of the Cherenkov radiation seem to support these new estimates.On the other hand, simulations of the fluorescence light production show rather wide distribution with respect to the shower axis.

7 Acknowledgements

We thank G.T. Zatsepin for useful discussions, INTAS (grant 03-51-5112), RFBR (grant 05-02-17410) and LSS-5573.2006.2.

References

[1] K. Greizen, Phys. Rev. Lett. **16** (1966) 748.

[2] G.T. Zatsepin, V.A. Kuzmin, JETP Lett. **4** (1966) 78.

[3] M.I. Pravdin, A.V. Glushkov et al., Proc. of the 29th ICRC, Pune **7** (2005) 743.

[4] K. Shinozaki, M. Teshima, Nucl. Phys. B (Proc. Suppl.) **136** (2004) 18.

[5] D.R. Bergman et al., Proc. of the 29th ICRC, Pune **7** (2005) 315.

[6] P. Sommers et al., Proc. of the 29th ICRC, Pune **7** (2005) 387.

[7] L.G. Dedenko, G.F. Fedorova, E.Yu. Fedunin et al., Nucl. Phys. B (Proc. Suppl.) **136** (2004) 18.

[8] L.G. Dedenko et al., Nucl. Phys. B (Proc. Suppl.) **151** (2006) 19.

[9] D. Heck et al., Report FZKA, Forschungszentrum Karlsruhe **6019** (1998); http://www-ik.fzk.de/corsika/.

[10] The GEANT4 Collaboration, http://wwwinfo.cern.ch/asd/geant4.html/.

[11] M.N. Dyakonov, T.A. Egorov, A.N. Efimov et al., Proc. of the 20th ICRC, Moscow **5** (1987) 486.

[12] N.N. Kalmykov, S.S. Ostapchenko, Yad. Fiz. **56** (1993) 105; Phys. At. Nucl. **3** (1993) 56.

[13] G. Lefeuvre et al., Proc. of the 29th ICRC, Pune **8** (2005) 37.

[14] D. Gora et al., Proc. of the 29th ICRC, Pune **7** (2005) 191.

[15] P. Homola et al., astro-ph/0311442 (2003).

[16] A.B. Migdal, Phys. Rev. **103** (1956) 1811.

[17] A.V. Plyasheshnikov, F.A. Aharonyan, JPhG **28** (2002) 267.

[18] G.I. Rubtsov et al., Phys. Rev. (2006) in press.

[19] L.G. Dedenko, G.F. Fedorova, T.M. Roganova et al., Proc. of the 29th ICRC, Pune **7** (2005) 211.